Presented at the *Sixth International Symposium on Fire Safety Science*, Poitiers, France, July 1999

NUMERICAL MODELING OF COUNTERFLOW DIFFUSION FLAMES INHIBITED BY IRON PENTACARBONYL*

Marc D. Rumminger† and Gregory T. Linteris‡
Building and Fire Research Laboratory
National Institute of Standards and Technology, Gaithersburg MD 20899-8651, USA

ABSTRACT

This paper presents the first detailed numerical study of the extinction of methane-air counterflow diffusion flames by the super-effective agent iron pentacarbonyl. Calculations using a gas-phase chemical mechanism reproduce the magnitude of inhibition for small amounts of inhibitor in the air, but overpredict the inhibition effect for larger amounts of inhibitor. Reaction pathway and reaction flux analyses show that a catalytic cycle involving FeO, $Fe(OH)_2$, and FeOH is primarily responsible for catalytic recombination of H atoms which produces the inhibition, and that a new cycle involving Fe(OH), FeOOH and $Fe(OH)_2$ has a minor role. Reaction flux calculations demonstrate that the fractional flux of H and O atoms through the iron reactions increases as inhibitor concentration increases, but eventually the fractional fluxes level off. Saturation of the catalytic cycles can partially explain the diminishing effect of the inhibitor at high inhibitor loading shown in both the calculated and experimental results. Flame structure calculations are used to determine the reasons for stronger inhibition for air-side addition of the inhibitor than for fuel-side. Simulations using a idealized inhibitor confirm the important role of transport in inhibition of counterflow diffusion flames.

KEYWORDS: halon alternatives, diffusion flames, flame inhibition, modeling, iron pentacarbonyl

INTRODUCTION AND BACKGROUND

Production of the effective and widely-used fire suppressant CF_3Br (and similar compounds) has been banned because of its role in the destruction of stratospheric ozone. Although replacement agents (mostly hydrofluorocarbons) are being developed, an agent with all of the desirable properties of CF_3Br is proving difficult to find, and research has intensified. There exist metallic compounds which are up to 100 times more effective than the brominated

---

* Official contribution of NIST, not subject to copyright in the United States
† National Research Council/NIST postdoctoral fellow
‡ Corresponding author. e-mail: linteris@nist.gov

agents [1-3]. In particular, iron pentacarbonyl ($Fe(CO)_5$) has been found to be one of the strongest inhibitors [4]. Although $Fe(CO)_5$ is highly toxic and flammable, it is so effective that studying its kinetic behavior in flames could provide insight into its mechanism and those of other highly effective agents and allow development of efficient, non-toxic agents.

The strong inhibitory effect of iron pentacarbonyl was discovered in the 1960s by Wagner and co-workers [1],[4] who performed burning velocity and spectroscopic measurements in premixed hydrocarbon and hydrogen flames. Because of its strong inhibiting effect and the limited understanding of its inhibition chemistry, iron pentacarbonyl is the subject of increasing attention [5-8]. Recent experiments have examined the behavior of iron pentacarbonyl in premixed methane-oxygen-nitrogen flames and in counterflow diffusion flames [5]. In premixed flames, the experiments showed that while small amounts of $Fe(CO)_5$ reduce the flame speed proportionally to the amount of inhibitor, increasing the inhibitor concentration above a certain amount had virtually no effect. The authors postulated that the lack of further inhibition was due to condensation of active gas-phase species to relatively inactive particles.

Based on work of Jensen and Jones [9], a gas-phase kinetic description of flame inhibition has been developed and used for understanding $Fe(CO)_5$ inhibition of premixed methane flames with varying oxygen mole fraction [8] and temperature [7], and for predicting the global properties (extinction) of diffusion flames [8]. The calculations predicted many (but not all) of the features, implied that inhibition occurs through gas-phase chemistry, and again indicated that condensation of active species may be important. Flame simulations using the chemical mechanism in Ref. [8] have primarily concerned premixed flames. Although study of premixed flames can provide great insight into inhibition chemistry, the study of diffusion flames—which are more representative of real fires—is required as well.

Most of the previous fundamental studies of flame inhibition have also been performed in premixed flames (due to the simplicity of interpretation of the results), but a substantial amount of work has also been done in diffusion flames. The counterflow configuration has been frequently used because of its flexibility, unambiguous extinction condition, and amenability to numerical modeling. Most of the early counterflow diffusion flame research involved experiments on halogenated inhibitors with some analysis [10-12]. Recent work has involved both experiments and numerical modeling [13-17]. Study of super-effective inhibitors in diffusion flames has been limited to $Fe(CO)_5$ [5, 6] and dimethyl methylphosphonate [18, 19].

An important finding of previous inhibited diffusion flame research is the dependence of the inhibitor's effectiveness on the location of agent addition (fuel or oxidizer stream) [5, 10, 12, 15-18]. Although all researchers find that much higher agent mole fractions are required in the fuel stream than the oxidizer stream for extinction, some find that most of the discrepancy is accounted for by the differing mass flux of agent to the reaction zone [12, 15], while others find additional differences even after accounting for these effects [16, 18]. As described by Fallon et al. [17], addition of reactive inhibitors can alter the flame location, changing the effective flow-field residence time for a given value of the strain rate; consequently, they stressed the use of scalar dissipation rate as the relevant extinction parameter rather than the

strain rate when these effects are important. In contrast to the above results, Ibiricu and Gaydon [20] usually found the strongest effect on total OH emission when agents were added to the fuel stream. Despite the large number of studies, none of them rigorously addressed differences in the chemical interactions of the inhibitor with other species in the primary heat release zone of the flame when the agent is introduced from different sides of the diffusion flame, and none have numerically modeled inhibition by the most powerful agents.

This paper describes the first detailed numerical study of the extinction of counterflow *diffusion* flames by a super-effective agent. A recently developed chemical kinetic mechanism of iron species inhibition of hydrocarbon flames is used to investigate the causes and limitations of the inhibition, and implications for other agents are discussed.

APPROACH

The present paper analyzes in detail the experimental results for the $Fe(CO)_5$-inhibited diffusion flames of Ref. [5]. The counterflow diffusion flame in that work consisted of opposing jets of fuel and oxidizer. Since examination of the numerical results shows that addition of the inhibitor at the mole fractions of the study does not change the flame location (defined by the point of peak temperature), the extinction condition was characterized by the strain rate (the maximum velocity gradient on the air side of the flame). Although techniques such as laser Doppler velocimetry (LDV) are the most accurate method of determining strain rate, LDV seeding particles could affect the condensation of the iron species. Therefore, an analytical approximation [21] was used to quantify the strain rate at extinction since it has been found to be an acceptable approximation [22]. Since absolute values of the extinction strain rate a_{ext} depend upon the flow-field description, whereas trends in a_{ext} are independent of these [22], we normalize a_{ext} by the value for the equivalent uninhibited flame.

Numerical calculations are used to understand the powerful inhibition of $Fe(CO)_5$ in the counterflow diffusion flame. The equations of mass, momentum, and energy conservation are solved using a numerical code developed by Smooke [23], which uses the *Chemkin*[§] [24] and the transport property subroutines [25]. The potential flow boundary condition is used in the calculations. A one-carbon mechanism [26] (17 species and 52 chemical reactions) serves as a description of the methane oxidation. The chemical mechanism for $Fe(CO)_5$ inhibition of flames (12 species and 55 reactions), and necessary thermodynamic data, are compiled from a variety of sources and are summarized in Ref. [8]. All calculations and experiments describe flames at one atmosphere pressure, with $Fe(CO)_5$ added to either the fuel or oxidizer stream in concentrations of up to 500 ppm (all uses of ppm in this paper signify mole fraction $\cdot 10^6$).

In this paper, calculations of counterflow flames are compared with the experimental measurements of Ref. [5]. Although all six of the test cases in Ref. [5] are of interest, space

[§] Certain commercial equipment, instruments, or materials are identified in this paper to adequately specify the procedure. Such identification does not imply recommendation or endorsement by the National Institute of Standards and Technology, nor does it imply that the materials or equipment are necessarily the best available for the intended use.

limitations force us to restrict the discussion in this paper to two cases: a typical methane-air counterflow flame with $Fe(CO)_5$ added to either the air or fuel stream. In order to gain insight into the inhibition mechanism, we discuss the flame structure of uninhibited and inhibited flames, radical production in inhibited flames, reaction pathways for iron species, and differences between addition of inhibitor to the fuel and air side. Finally, calculations are performed with an idealized 'perfect' inhibitor to examine limitations to flame inhibition in diffusion flames.

RESULTS AND DISCUSSION

Figure 1 shows the calculated flame structure for CH_4 flowing against air, with a strain rate within 0.1% of the extinction strain rate. The stagnation plane, where the two jet flows converge and the velocity is zero, is at x=0.0 cm. The peak temperature is found on the air side of the stagnation plane, about 0.1 cm away. The fuel molecules must diffuse across the stagnation plane to reach the oxidizer. The mole fraction profiles in the plot show that there is significant leakage of O_2 into the fuel zone, and some CH_4 leakage into the air side of the flame. The mole fraction profiles of H_2O, CO_2 and CO are similar in shape to the temperature profile. The peaks of the chain carriers O, H, and OH are on the air side of the flame, and the magnitude is about equal for O and H (in contrast to a premixed flame where [H] is about twice that of [O]). These factors have important implications for flame inhibition, as is described below.

Air-Side Addition of $Fe(CO)_5$

The flame considered in this section is methane and air with $Fe(CO)_5$ added to the air stream. As in the uninhibited case of Figure 1, the flame is located on the air side of the stagnation plane. The measured [5] and calculated normalized extinction strain rate as a function of the input

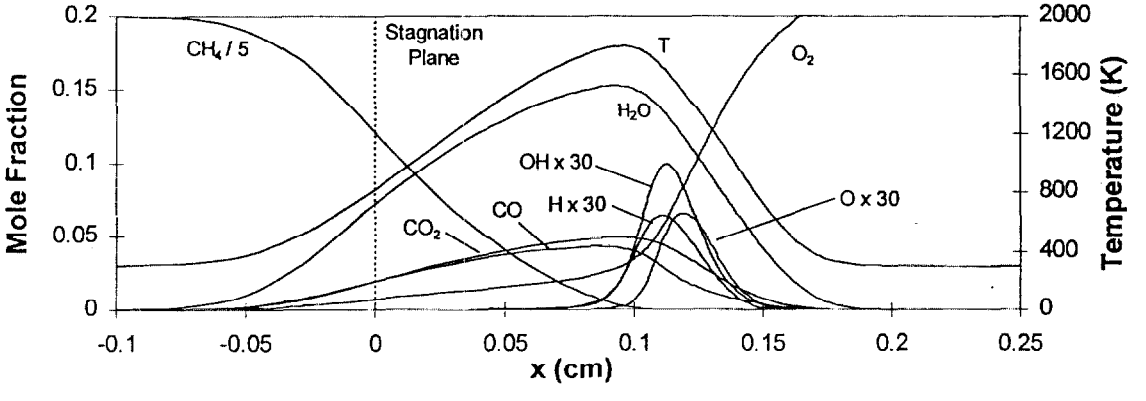

FIGURE 1: Calculated flame structure for a CH_4 vs. air flame near extinction (a=522 s^{-1}). The stagnation plane is noted by the line at x = 0. Fuel jet location (x_f) = -0.41 cm, air jet location (x_{air}) = 0.59 cm.

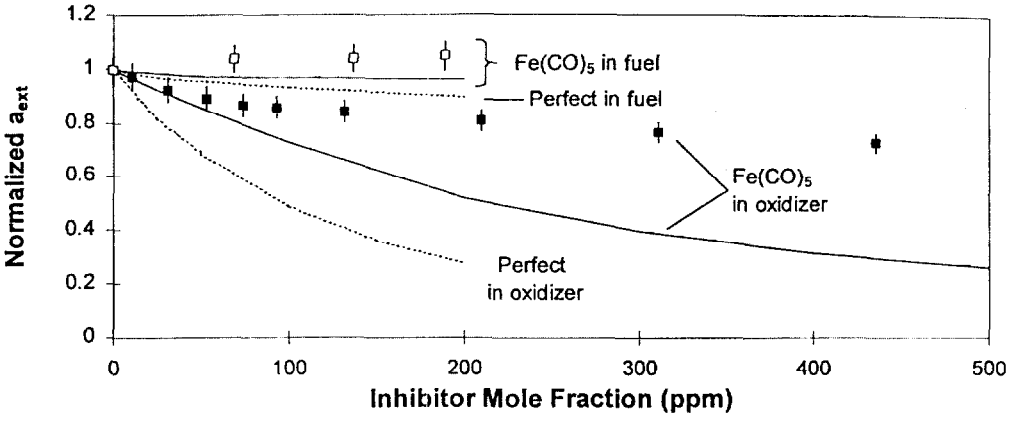

FIGURE 2: Normalized extinction strain rate for counterflow diffusion flames. Closed symbols: measurements with the $Fe(CO)_5$ in the oxidizer; open symbols: measurements with $Fe(CO)_5$ in the fuel; solid lines: calculations with $Fe(CO)_5$; dashed lines: calculation with perfect inhibitor. Data from Ref. [5].

$Fe(CO)_5$ mole fraction (X_{in}) are shown in Figure 2 (the dashed lines are discussed in a later section). The uncertainty of the normalized extinction strain rate measurement is ±5% [5]. For this flame, the calculated maximum temperature is approximately 1800 K at extinction. For the uninhibited flame, the measured a_{ext} is 610 ± 30 s^{-1} and the calculated a_{ext} is 522 s^{-1}. Experimental results show that when $Fe(CO)_5$ is added to the oxidizer stream a significant decrease in a_{ext} results; in contrast, addition to the fuel stream produces little change in a_{ext}. The numerical calculations qualitatively describe this behavior, and they also accurately predict the magnitude of the inhibition at low values of X_{in}. For higher values of X_{in}, the model predicts too much inhibition; this discrepancy has been hypothesized to be the result of condensation, which removes inhibiting gas-phase species from the flame zone [5, 8].

For the case in which the inhibitor is added to the air, we now examine the flame structure (Figure 3). The temperature profile in the inhibited flame is broadened because of the lower strain rate, and the peak is shifted slightly towards the air side relative to the uninhibited case (roughly 0.05 cm). For flames with identical strain rates, the addition of $Fe(CO)_5$ has no noticeable effect on the temperature profile, except very close to a_{ext}. The $Fe(CO)_5$ decomposes near 800 K and the products are converted to the inhibiting species (FeOH, $Fe(OH)_2$ and FeO). The regions of high iron species mole fractions correspond to the region of high H- and O-atom mole fraction, which allows the iron species to scavenge radicals. Indeed, detailed examination of the reaction rate profiles shows that the depression in the $Fe(OH)_2$ profile and the lack of a sharp peak in the FeOH profile are caused by their rapid reaction with H atoms, while the depression in the FeO_2 curve is from its reaction with O atoms.

Next, we examine the effect of $Fe(CO)_5$ on the maximum flame temperature, and O and H mole fraction as strain rate varies. In Figure 4, the calculated temperature is shown as a function of strain rate for a given value of inhibitor loading (X_{in} from 0 to 200 ppm). The point in each curve with highest strain rate represents the extinction point. For a given value

of X_{in}, increasing the strain reduces the peak temperature, since the heat release then becomes kinetically limited; likewise, for a given strain, increasing X_{in} also decreases the peak temperature. Although this reduction in temperature may seem inconsistent with the idea that $Fe(CO)_5$ is a purely chemical inhibitor [27], slowing the overall reaction rate reduces the heat released in the limited time available in the flow system in the same way that limiting the time for reaction (by increasing the strain) also limits the extent of reaction. The overall reaction rate is lowered as the inhibitor reduces the radical populations, which slows the oxidation of carbon monoxide. Comparing the extinction point for each inhibitor concentration (Figure 4), it is interesting that the temperature at extinction is *higher* in the inhibited flames than the uninhibited flames. This result is consistent with recent counterflow calculations for halogenated agents [28].

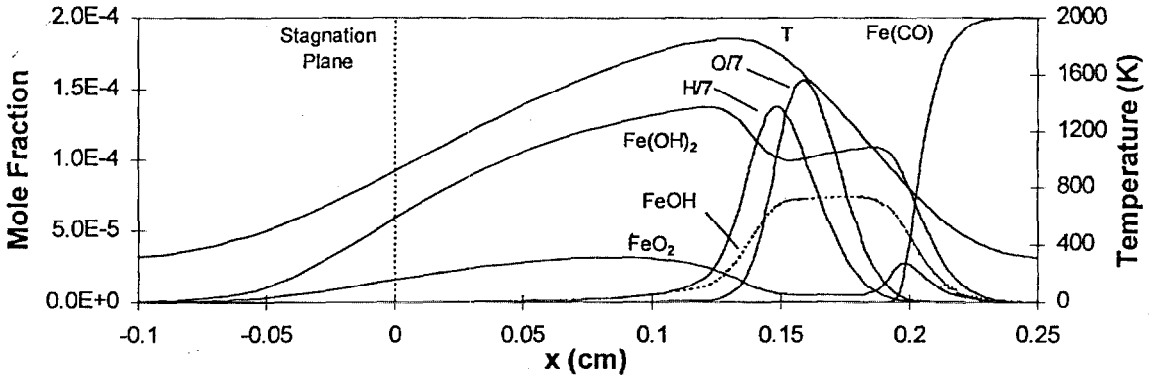

FIGURE 3: Iron species, O, H, and temperature with 200 ppm inhibitor in the air, near extinction (a= 257 s^{-1}). The stagnation plane is noted by the line at $x = 0$. $x_f = -0.4$ cm, $x_{air} = 0.6$ cm.

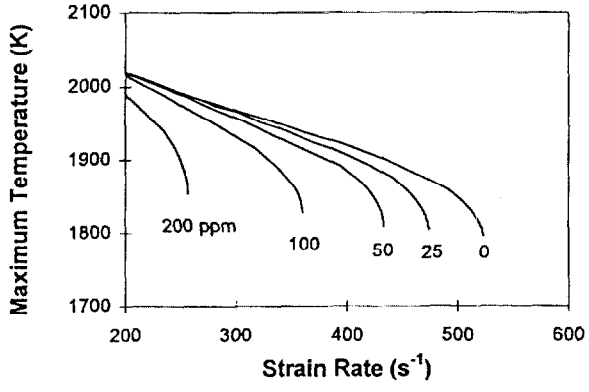

FIGURE 4: Maximum flame temperature vs. strain rate for X_{in} between 0 and 200 ppm.

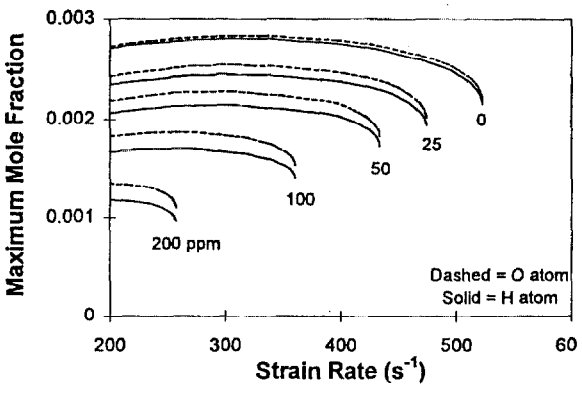

FIGURE 5: Maximum mole fraction for H and O vs. strain rate for X_{in} between 0 and 200 ppm.

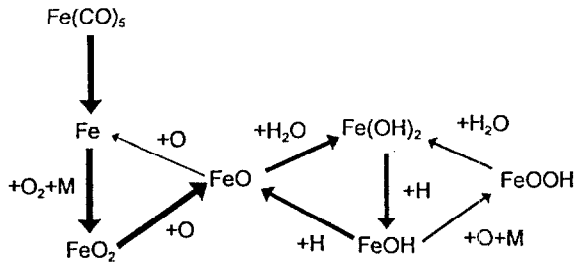

FIGURE 6: Reaction pathways in CH_4 vs. air flames with inhibitor in the air. Thicker arrows correspond to higher importance. Reaction partners are next to each arrow.

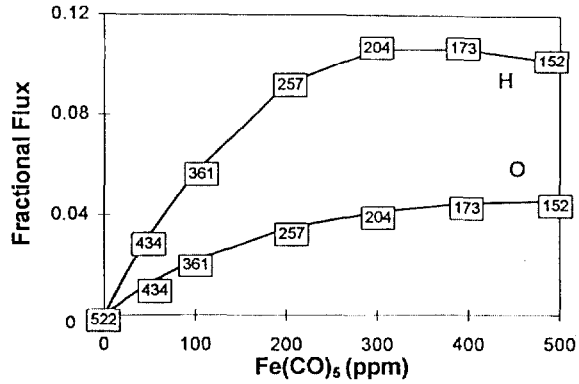

FIGURE 7: Fractional H- and O-atom flux through key iron reactions for flames near the extinction point. The numbers at each point refer to a_{ext} (in s^{-1}) at that X_{in}.

The calculated reduction of radical mole fraction caused by $Fe(CO)_5$ is shown in Figure 5. For a given value of X_{in}, as the strain rate increases, the O- and H-atom peak mole fractions do not change significantly until just near extinction, when they drop rapidly. For a given strain rate, however, a small addition of inhibitor causes a sharp reduction in the peak radical mole fractions. For example, addition of 200 ppm reduces the peak radical mole fractions by roughly 50% (for strain rates below 250 s^{-1}). In premixed flames, the strong reduction of H-atoms has been found to be the result of a catalytic cycle involving FeO, FeOH and $Fe(OH)_2$ which converts H atoms into less reactive H_2 molecules [9] (the O-atom mole fraction decreases due to fast H_2-O_2 shuffle reactions). It is of interest to determine if the same catalytic cycle is responsible for the reduced radical mole fractions in the present counterflow diffusion flame.

A reaction pathway analysis is useful for elucidating the important reactions for flame inhibition. Figure 6 presents the destruction pathway for $Fe(CO)_5$ and its reaction products in the counterflow flame, as generated by the graphical post-processing program *Xsenkplot* [29]. Since the figure is based on analysis of flames with multiple strain rates and multiple X_{in}, it is meant to be qualitative only. The thickness of the arrow corresponds to the relative importance of the reaction.

Upon heating, the $Fe(CO)_5$ decomposes in several steps (shown as a single step for simplicity), leaving Fe and CO. The Fe reacts with O_2 to form FeO_2, which then reacts with O to form FeO. The bulk of the FeO reacts with water to begin a catalytic cycle that converts H atoms into less reactive H_2 molecules, as described by

$$FeO + H_2O \leftrightarrow Fe(OH)_2$$
$$Fe(OH)_2 + H \leftrightarrow FeOH + H_2O$$
$$FeOH + H \leftrightarrow FeO + H_2$$

Additionally, a portion of the reactions occur through a cycle involving FeOOH, FeOH, and

$Fe(OH)_2$ in which the net result is $O+H \leftrightarrow OH$. This cycle is not important for premixed CH_4-air flames [8], where the O atom population is much smaller than the H atom population. In counterflow diffusion flames, however, the peak mole fraction of O and H atom are nearly equal, which increases the importance of the FeOH+O reaction. It should be noted that while the peak O and H mole fractions at extinction are typically reduced by about a factor of two at X_{in} = 200 ppm, peak OH is lowered much less, possibly because it is created by the cycle described above. Further, the high O atom population in the diffusion flame leads to an additional minor catalytic cycle in which FeO reacts with O to reform Fe thus completing a cycle that results in $O+O \leftrightarrow O_2$.

We further examine the inhibition effect using the technique of reaction flux analysis. We measure the relative importance of the iron reactions by calculating the fraction of H-atom and O-atom consumption that occurs through each reaction shown in Figure 6. To calculate the reaction flux, the rate of each reaction consuming an H or O atom is determined at each location in the flame and then the resulting reaction rate profile is integrated over the entire flame. The contribution of each reaction to the total consumption is the "fractional flux" of the species through that particular reaction. More details about the technique can be found in Ref. [30].

The diminishing effectiveness of $Fe(CO)_5$ at high X_{in} shown in Figure 2 may be partially explained by Figure 7, which plots the fractional flux of H and O through key iron reactions as X_{in} varies. The calculations are for flames nearly at extinction, and the figure includes the actual extinction strain for that value of X_{in}. At low values of X_{in} the fractional flux through the iron reactions increases linearly, but beyond 100 ppm, the rate of increase begins to slow. At high X_{in} the catalytic cycles become 'saturated' [8]: increasing X_{in} does not lead to a proportionally greater fraction of the radicals being recombined by the iron species. For a 67% increase in the mole fraction of $Fe(CO)_5$ from 300 to 500 ppm, the *total* destruction flux of either H or O through the iron cycles increases about 15%. However, as Figure 7 shows, the *fractional* flux of O atom increases by just 10%, while it decreases for H atom. The decrease in H atom fractional flux is caused by an increase in total destruction flux for X_{in} > 300 ppm. In particular, a large increase in the forward and reverse rates of $CH_4+H \leftrightarrow CH_3+H_2$ occurs due to more overlap of CH_4 with regions of high H-atom mole fraction. Although saturation of the catalytic cycles is a partial explanation for the reduced effectiveness at higher X_{in}, the loss of effectiveness is not fully understood, in part because the numerical model does not include particle formation. Experimental measurements of particles in $Fe(CO)_5$-inhibited flames could improve understanding of the reduced effectiveness.

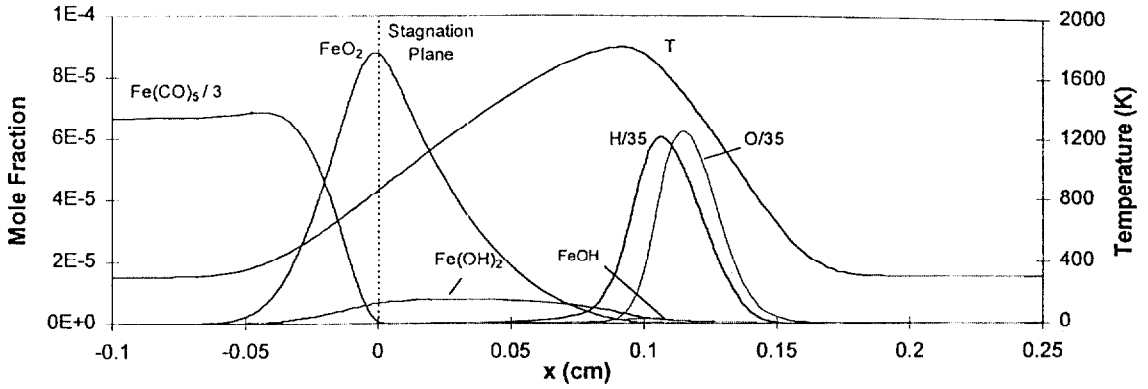

FIGURE 8: Iron species, O atom, H atom, and temperature for flame on the air side, 200 ppm inhibitor in the fuel, near extinction (a = 496 s^{-1}). The stagnation plane is noted by the line at $x = 0$. $x_f = -0.4125$ cm, $x_{air} = 0.5875$ cm.

Fuel-Side Addition of $Fe(CO)_5$

Recall that addition of inhibitor to the fuel results in far less inhibition than addition to the oxidizer (Figure 2). Calculations of flame structure, in which the chemistry and transport of the inhibitor is considered, can provide great insight into the reasons for the difference. Figure 3 showed that when the inhibitor is in the oxidizer, there is significant interaction between the iron species and the radicals. With addition of 200 ppm of $Fe(CO)_5$ to the fuel (Figure 8), however, the distribution of species is significantly different: the $Fe(CO)_5$ in the fuel stream decomposes, the decomposition products react to form FeO_2, but little of this species is able to diffuse to the region of high O atom to form FeO. Although this result implies that diffusion of the inhibitor to the reaction zone is the controlling process, the result is more subtle: both transport to the correct location and reaction (of FeO_2) with the proper species (O) is necessary to form the inhibiting intermediate (FeO). (In the present flame, however, the limitation is actually transport only. This is demonstrated by a calculation in which 200 ppm of FeO, instead of $Fe(CO)_5$, is added to the fuel. The exchange results in only a 2% additional reduction in extinction strain rate.)

Although elimination of one of the steps in formation of the inhibiting species can partially separate the chemistry and transport effects, simulating a 'perfect inhibitor' can provide further insight. A perfect inhibitor is one that enters the flame as an inhibiting species, does not decompose at high temperature, scavenges radicals at gas kinetic rates, and regenerates itself. Babushok et al. [27] developed a model for such an inhibitor and used it to investigate the upper limits of chemical inhibition in premixed flames. The thermodynamic and transport properties are those of argon. Although highly idealized, the perfect inhibitor can be used to differentiate between chemical and transport effects in counterflow flames.

We now return to Figure 2, which shows calculated normalized extinction strain rates with addition of the perfect inhibitor to the oxidizer or fuel. As in the case of $Fe(CO)_5$, addition to the oxidizer has a much stronger effect than addition to the fuel. This difference remains despite the fact that neither decomposition nor formation of inhibiting species is required for

the perfect inhibitor. Calculations of flame structure for the flames with perfect inhibitor in the fuel show results similar to those described above for $Fe(CO)_5$: when added to the fuel, the inhibiting species cannot reach the region of high H and O atoms. Increasing the diffusivity of the perfect inhibitor results in more inhibition, but still far less than for inhibitor addition to the oxidizer.

These conclusions apply to the methane-air diffusion flame with a distance of about 1 mm between the flame and the stagnation plane. For mixtures in which the flame is closer to the stagnation plane (a heavier fuel molecule, for example), there may be more inhibition caused by fuel-side addition of an inhibitor.

CONCLUSION

This paper presents the first detailed numerical study of the extinction of counterflow methane-air diffusion flames by a super-effective chemical inhibitor, $Fe(CO)_5$. The normalized extinction strain rate for agent addition to the air stream is well-predicted by the numerical calculations for low inhibitor concentration, and the vastly different behavior for fuel- vs. air-side addition is predicted by the model. The calculations show that at a given strain rate, the flame temperature decreases as X_{in} increases, and that the maximum mole fraction of H and O decrease sharply as X_{in} increases. For flames near the extinction, the peak temperature increases as X_{in} increases.

Reaction pathway and reaction flux analyses show that a catalytic cycle that scavenges H atoms is responsible for most of the inhibition, and a new cycle involving FeOOH has an additional, but minor, role. Reaction flux calculations demonstrate that the fractional flux of H and O atoms consumed through catalytic recombination cycles involving the iron species increases linearly as X_{in} increases up to about 100 ppm, and that above about 300 ppm, the cycles do not account for an increasing fraction of the H-atom consumption.

We have presented the first detailed kinetic comparison of the difference between fuel-side and air-side addition of a super-effective inhibitor. Our calculations show that addition of $Fe(CO)_5$ to the fuel side of a methane-air counterflow diffusion flame has little effect because an insignificant amount of the inhibiting species reaches the region of high radical mole fraction, and thus cannot enter into the catalytic cycles. Perfect inhibitor calculations show that even an idealized 'perfect inhibitor' does not have a strong inhibition effect when added to the fuel in a methane-air counterflow flame. This further supports the idea that transport of the inhibiting species to the region of high radical mole fraction is critical.

Future work still remains on exploring $Fe(CO)_5$'s behavior in other types of diffusion flames, such as when the flame is on the fuel side of the stagnation plane, or when the flame is closer to the stagnation plane. Measurements of the rates of the key reactions in the catalytic cycles, as well as particle measurements in inhibited flames would provide important data to improve understanding of the inhibition mechanism of iron pentacarbonyl.

REFERENCES

1. Lask, G. and Wagner, H. G., "Influence of Additives on the Velocity of Laminar Flames," Eighth Symposium (International) on Combustion, pp.432-438, 1962.
2. Miller, D. R., Evers, R. L., and Skinner, G. B., "Effects of Various Inhibitors on Hydrogen-Air Flame Speeds," Combustion and Flame, 7, 137, 1963.
3. Vanpee, M. and Shirodkar, P., "A Study of Flame Inhibition by Metal Compounds," Seventeenth Symposium (International) on Combustion, pp.787-795, 1979.
4. Bonne, U., Jost, W., and Wagner, H. G., "Iron Pentacarbonyl in Methane-Oxygen (or Air) Flames," Fire Research Abstracts and Reviews, 4, 6, 1962.
5. Reinelt, D. and Linteris, G. T., "Experimental Study of the Inhibition of Premixed and Diffusion Flames by Iron Pentacarbonyl," Twenty-Sixth Symposium (International) on Combustion, pp.1421-1428, 1996.
6. Skaggs, R. R., McNesby, K. L., Daniel, R. G., Homan, B., and Miziolek, A. W., "Measurement of Hydroxyl Radical during Suppression of Low Pressure Opposed Flow Methane/Air Diffusion Flames by $Fe(CO)_5$, CF_3Br, and N_2 ," Halon Options Technical Working Conference, pp.121-133, 1998.
7. Rumminger, M. D., Reinelt, D., Babushok, V., and Linteris, G. T., "Inhibition of Flames by Iron Pentacarbonyl," Halon Options Technical Working Conference, pp.145-156, 1998.
8. Rumminger, M. D., Reinelt, D., Babushok, V., and Linteris, G. T., "Numerical Study of the Inhibition of Premixed And Diffusion Flames by Iron Pentacarbonyl," Combustion and Flame, 116, 207, 1999.
9. Jensen, D. E. and Jones, G. A., "Catalysis of Radical Recombination in Flames by Iron," Journal of Chemical Physics, 60, 3421, 1974.
10. Milne, T. A., Green, C. L., and Benson, D. K., "The Use of the Counter-Flow Diffusion Flame in Studies of Inhibition Effectiveness of Gaseous and Powdered Agents," Combustion and Flame, 15, 255, 1970.
11. Seshadri, K. and Williams, F. A., "Effect of CF_3Br on Counterflow Combustion of Liquid Fuel with Diluted Oxygen" in Halogenated Fire Suppressants , ed. R.G. Gann, pp. 149-182, American Chemical Society, Washington, D.C., 1975.
12. Niioka, T., Mitani, T., and Takahashi, M, "Experimental Study on Inhibited Diffusion and Premixed Flames in a Counterflow System," Combustion and Flame, 50, 89, 1983.
13. Chelliah, H. K, Yu, G., Hahn, T. O., and Law, C. K, "An Experimental and Numerical Study on the Global and Detailed Kinetics of Premixed and Nonpremixed Flames of Chloromethane, Methane, Oxygen and Nitrogen," Twenty-Fourth Symposium (International) on Combustion, pp.1083-1090, 1993.
14. Hamins, A., Trees, D., Seshadri, K., and Chelliah, H. K., "Extinction of Nonpremixed Flames With Halogenated Fire Suppressants," Combustion and Flame, 99, 221, 1994.
15. Masri, A. R., "Chemical Inhibition of Nonpremixed Flames of Hydrocarbon Fuels With CF_3Br," Combustion Science and Technology, 96, 189, 1994.
16. Trees, D., Grudno, A., and Seshadri, K., "Experimental and Numerical Studies on Chemical Inhibition of Nonpremixed Methane Flames by CF_3Br," Combustion Science and Technology, 124, 311, 1997.
17. Fallon, G. S., Chelliah, H. K, and Linteris, G. T., "Chemical Effects of CF_3H in Extinguishing Counterflow CO/Air/H_2 Diffusion Flames," Twenty-Sixth Symposium

(International) on Combustion, pp.1395-1403, 1996.
18. MacDonald, M. A., Jayaweera, T. M., Fisher, E. M., and Gouldin, F. C., "Variation of Chemically Active and Inert Flame-Suppression Effectiveness with Stoichiometric Mixture Fraction," Twenty-Seventh Symposium (International) on Combustion, 1998, in press.
19. MacDonald, M. A., Jayaweera, T. M., Fisher, E. M., and Gouldin, F. C., "Inhibition of Nonpremixed Flames by Phosphorous-Containing Compounds," Combustion and Flame, 116, 166, 1999.
20. Ibiricu, M. M. and Gaydon, A. G., "Spectroscopic Studies of the Effect of Inhibitors on Counterflow Diffusion Flames," Combustion and Flame, 8, 51, 1964.
21. Seshadri, K. and Williams, F. A., "Laminar Flow between Parallel Plates with Injection of Reactant at High Reynolds Number," Int. J. of Heat and Mass Transfer, 21, 137, 1978.
22. Chelliah, H. K, Law, C. K, Ueda, T, Smooke, M. D, and Williams, F. A., "An Experimental and Theoretical Investigation of the Dilution, Pressure and Flow-Field Effects on the Extinction Condition of Methane-Air-Nitrogen Diffusion Flames," Twenty-Third Symposium (International) on Combustion, pp.503-511, 1991.
23. Smooke, M. D, Puri, I. K, and Seshadri, K., "A Comparison between Numerical Calculations and Experimental Measurements of the Structure of a Counterflow Diffusion Flame Burning Diluted Methane in Diluted Air," Twenty-First Symposium (International) on Combustion, pp.1783-1792, 1986.
24. Kee, R. J., Rupley, F. M., and Miller, J. A., "CHEMKIN-II: A Fortran Chemical Kinetics Package for the Analysis of Gas Phase Chemical Kinetics", Sandia National Laboratory, SAND89-8009B, 1989.
25. Kee, R. J., Dixon-Lewis, G., Warnatz, J., Coltrin, R. E., and Miller, J. A., "A Fortran Computer Package for the Evaluation of Gas-Phase, Multicomponent Transport Properties", Sandia National Laboratory, SAND86-8246, 1986.
26. Peters, N., "Flame Calculations with Reduced Mechanisms - An Outline" in Reduced Kinetic Mechanisms for Applications in Combustion Systems , ed. Peters, N. and Rogg B., pp. 3-14, Springer-Verlag, New York, 1993.
27. Babushok, V., Tsang, W., Linteris, G. T., and Reinelt, D., "Chemical Limits to Flame Inhibition," Combustion and Flame, 115, 551, 1998.
28. Lentati, A. M. and Chelliah, H. K, "Physical, Thermal and Chemical Effects of Fine-Water Droplets in Extinguishing Counterflow Diffusion Flames," Twenty-Seventh Symposium (International) on Combustion, 1999, in press.
29. NIST, XSenkplot, An Interactive, Graphics Postprocessor for Numerical Simulations of Chemical Kinetics, http://www.nist.gov/cstl/div836/xsenkplot , 1997.
30. Rumminger, M. D. and Linteris, G. T., "Inhibition of Premixed Carbon Monoxide-Hydrogen-Oxygen-Nitrogen Flames by Iron Pentacarbonyl," submitted to *Combustion and Flame*, March 1999.